Impulsive Events in the Evolution of a Forced Nonlinear System

D. W. Longcope and R. N. Sudan
Laboratory of Plasma Studies, Cornell University, Ithaca, New York 14853
(Received 4 November 1991)

Long-time numerical solutions of a low-dimensional model of the reduced MHD equations show that, when this system is driven quasistatically, the response is punctuated by impulsive events. The statistics of these events indicate a Poisson process; the frequency of these events scales as ΔE_M^{-1}, where ΔE_M is the energy released in one event.

PACS numbers: 52.30.−q, 52.35.−g, 96.60.Rd

When a nonlinear system is driven by external forces quasistatically, i.e., at a rate slower than the transit time of a signal across the system, $\tau = l/v_s$ (l is the typical scale length and v_s is the signal velocity), the response is also expected to be quasistatic. We show in this Letter, through a specific example, that this conclusion is not always valid. During the process of quasistatic evolution the system seeks to occupy a state of quasiequilibrium with minimum potential energy. If it so happens at some stage that the second variation of the potential energy [1] vanishes, i.e., $\delta^{(2)}W = 0$, the local equilibrium is lost and the system drops to a neighboring potential minimum if the third-order potential energy $\delta^{(3)}W < 0$. The time scale of this transition is determined by the internal dynamics of the system and not by the external forces. Thus, the general response of a nonlinear system is predicted to be periods of quasistatic evolution punctuated by abrupt impulsive events [2] whose time scale is of order τ. We investigate here the statistics of such abrupt impulsive events for a system with many degrees of freedom.

Solar flares [3] are an example of sporadically occurring impulsive events in nature. These occur on many scales of energy output ranging through microflares [4] and nanoflares [5]. Our present understanding postulates that the magnetic energy stored in coronal magnetic loops is released abruptly during a flare in the form of x rays, energetic particles, ejected mass, etc. Since the magnetic-field lines of a coronal loop are anchored in the dense photosphere the turbulent motions of the photosphere continually twist and untwist the field lines, thereby storing magnetic energy in the loop on average. In what follows, we develop a model that, in particular, should be applicable to microflares and nanoflares. The conclusions, however, may be more general and applicable to other systems where energy is stored on the long time scale but released in rapid events.

By ignoring curvature and gravitational stratification a coronal loop of length L can be mapped to a slab-shaped domain bounded with conducting planes at $z = 0$ and $z = L$ representing the photosphere [6]. The initial magnetic field in the loop is uniform, $\mathbf{B} = B_0\hat{\mathbf{z}}$. The two-dimensional velocity field at $z = 0$ and $z = L$ is specified. This motion is much slower than $\tau = L/v_A$, where v_A is the Alfvén velocity in the loop. The transverse dimension of the loop $a \ll L$. In this limit the magnetohydrodynamic equations describing the coronal plasma can be approximated by the so-called "reduced MHD" set of equations [7] that deal with vorticity $\Omega = \hat{\mathbf{z}}\cdot\nabla\times\mathbf{v}_\perp$ and the vector potential $A = \mathbf{A}\cdot\hat{\mathbf{z}}$:

$$\partial\Omega/\partial t + \mathbf{v}_\perp\cdot\nabla_\perp\Omega = \partial J/\partial z + \mathbf{B}_\perp\cdot\nabla_\perp J + \nu\nabla_\perp^2\Omega\,, \tag{1}$$

$$\partial A/\partial t + \mathbf{v}_\perp\cdot\nabla_\perp A = -\partial\phi/\partial z + \eta\nabla_\perp^2 A\,, \tag{2}$$

with $\mathbf{v}_\perp = \hat{\mathbf{z}}\times\nabla\phi$, $\mathbf{B}_\perp = \nabla A\times\hat{\mathbf{z}}$, $\Omega = \nabla_\perp^2\phi$, and $J = -\nabla_\perp^2 A$. Equations (1) and (2) are expressed in units of τ, L, and $a/2\pi$. The photospheric drive is introduced by prescribing $\Omega(\mathbf{x}_\perp,t,z=0) = f^0(\mathbf{x}_\perp,t)$, $\Omega(\mathbf{x}_\perp,t,z=1) = f^1(\mathbf{x}_\perp,t)$ to be randomly generated fields with Gaussian statistics and specified correlation time τ_C and root-mean-squared amplitudes τ_E^{-1}. This forcing is maintained quasistatic by demanding $\tau_E, \tau_C \gg 1$.

The set of reduced MHD equations (1) and (2) have been solved numerically and shown to lead to equilibria of increasing spatial complexity [2]. Numerical simulations capable of resolving this complexity are prohibitively expensive to run for long times so we will use a low-dimensional analog of the reduced MHD equations. This relatively simple set of 21 ordinary differential equations can be derived systematically in two steps. As a first step the perpendicular spatial dependence of all the scalar fields in (1) and (2) will be represented using only three orthogonal basis functions, $\psi_1(\mathbf{x}_\perp) = \sqrt{2}\cos(x)/\alpha$, $\psi_2(\mathbf{x}_\perp) = \sqrt{2}\cos(\alpha y)/\alpha$, and $\psi_3(\mathbf{x}_\perp) = 2\sin(x)\sin(\alpha y)/\alpha$, where α is a fixed parameter taken to be 0.8 in all that follows. In representing a scalar field, such as current, each basis function is multiplied by a coefficient depending on the third spatial coordinate z in addition to time. To simplify notation, these three coefficients can be combined into an isovector $\mathbf{J}(z,t)$.

Projecting Eqs. (1) and (2) onto these basis functions yields a set of six coupled partial differential equations in one dimension:

$$\partial\boldsymbol{\Omega}/\partial t + \boldsymbol{\phi}\times\boldsymbol{\Omega} = \partial\mathbf{J}/\partial z - \mathbf{A}\times\mathbf{J} - \nu\underline{\mathbf{L}}\cdot\boldsymbol{\Omega}\,, \tag{3}$$

$$\partial\mathbf{A}/\partial t + \boldsymbol{\phi}\times\mathbf{A} = -\partial\boldsymbol{\phi}/\partial z - \eta\underline{\mathbf{L}}\cdot\mathbf{A}\,, \tag{4}$$

where $\boldsymbol{\Omega} = -\underline{\mathbf{L}}\cdot\boldsymbol{\phi}$, $\mathbf{J} = \underline{\mathbf{L}}\cdot\mathbf{A}$, and the linear operator $\underline{\mathbf{L}}$ is the projection of the diffusion operator $-\nabla_\perp^2$ given by the diagonal matrix $\underline{\mathbf{L}} = \mathrm{diag}\{1,\alpha^2,1+\alpha^2\}$. The cross product appearing in each nonlinearity is the analog of the two-dimensional Poisson bracket often used when writing the reduced MHD equations.

To complete the derivation of the low-dimensional

model the current and vorticity will be represented on alternating points of a uniform grid in z. The spacing between points will be $\Delta z = \frac{1}{6}$ so the current isovectors, denoted $\mathbf{J}^0$, $\mathbf{J}^1$, $\mathbf{J}^2$, and $\mathbf{J}^3$, will appear at $z=0$, $\frac{1}{3}$, $\frac{2}{3}$, and 1, respectively; similarly the vorticities $\boldsymbol{\Omega}^1$, $\boldsymbol{\Omega}^2$, and $\boldsymbol{\Omega}^3$ are located at $z=\frac{1}{6}$, $\frac{1}{2}$, and $\frac{5}{6}$. In addition, vorticity must be prescribed at the ends, $z=0$ and 1, through two time-varying isovectors $\mathbf{f}^0$ and $\mathbf{f}^1$. This departure from the strict alternation between vorticity and current requires a modification of the standard centered difference scheme:

$$d\boldsymbol{\Omega}^n/dt+\boldsymbol{\phi}^n\times\boldsymbol{\Omega}^n=\tfrac{1}{2}(\Delta z)^{-1}(\mathbf{J}^n-\mathbf{J}^{n-1})-\tfrac{1}{2}\mathbf{A}^n\times\mathbf{J}^n-\tfrac{1}{2}\mathbf{A}^{n-1}\times\mathbf{J}^{n-1}-\nu\underline{\mathbf{L}}\cdot\boldsymbol{\Omega}^n, \quad (5)$$

$$d\mathbf{A}^0/dt+\boldsymbol{\phi}^1\times\mathbf{A}^0=-(\Delta z)^{-1}(\boldsymbol{\phi}^1+\underline{\mathbf{L}}^{-1}\cdot\mathbf{f}^0)-\eta\underline{\mathbf{L}}\cdot\mathbf{A}^0, \quad (6a)$$

$$d\mathbf{A}^n/dt+\tfrac{1}{2}(\boldsymbol{\phi}^{n+1}+\boldsymbol{\phi}^n)\times\mathbf{A}^n=-\tfrac{1}{2}(\Delta z)^{-1}(\boldsymbol{\phi}^{n+1}-\boldsymbol{\phi}^n)-\eta\underline{\mathbf{L}}\cdot\mathbf{A}^n,\quad n=1,2, \quad (6b)$$

$$d\mathbf{A}^3/dt+\boldsymbol{\phi}^3\times\mathbf{A}^3=(\Delta z)^{-1}(\underline{\mathbf{L}}^{-1}\cdot\mathbf{f}^1+\boldsymbol{\phi}^3)-\eta\underline{\mathbf{L}}\cdot\mathbf{A}^3. \quad (6c)$$

These equations are not intended to accurately approximate Eqs. (1) and (2), rather they are a low-dimensional analog of the full partial differential equations. In the system defined by Eqs. (5) and (6) the individual field line topology is not preserved; however, the magnetic flux is conserved.

The most important analogy between the two systems is their global energy balances. In each case the change in the total energy of the system (magnetic plus kinetic) equals the work done by the footpoints minus the viscous and Ohmic dissipation powers: $d(E_M+E_K)/dt=P_F-P_\nu-P_\eta$. In the low-dimensional system, (5) and (6), each of these quantities is a simple bilinear expression, such as

$$E_M=\tfrac{1}{4}\mathbf{A}^0\cdot\mathbf{J}^0+\tfrac{1}{2}\mathbf{A}^1\cdot\mathbf{J}^1+\tfrac{1}{2}\mathbf{A}^2\cdot\mathbf{J}^2+\tfrac{1}{4}\mathbf{A}^3\cdot\mathbf{J}^3,$$
$$P_F=\mathbf{f}^1\cdot\mathbf{A}^3-\mathbf{f}^0\cdot\mathbf{A}^0, \quad (7)$$
$$P_\nu=\nu\{|\boldsymbol{\Omega}^1|^2+|\boldsymbol{\Omega}^2|^2+|\boldsymbol{\Omega}^3|^2\}.$$

The other quantities, P_η and E_K, are non-negative expressions similar to E_M or P_η; only P_F can assume either sign.

The decay time for a stationary equilibrium, one with $\boldsymbol{\Omega}^n=0$, would be η^{-1}. In the coronal case this is as much as 10 orders of magnitude longer than a typical transit time so we will take $\eta=0$ in all that follows. On the other hand, oscillations about such an equilibrium (Alfvén waves) are expected to decay after several periods by one of a variety of mechanisms not present in the low-dimensional model [8,9]. Since viscosity is the only mechanism left in the model capable of doing this it will be retained as an effective Alfvén wave damping.

There are a wide range of equilibrium solutions to Eqs. (5) and (6) which can be distinguished by any one of their current isovectors; the isovector $\mathbf{J}^0$ will be used for this label. If such an equilibrium is perturbed by an infinitesimal internal displacement it will oscillate in a superposition of eighteen eigenmodes each of whose eigenfrequencies is either purely real or purely imaginary in the absence of viscosity. This follows from the self-adjointness of the energy functional, a property of (5) and (6) shared by both the full MHD and reduced MHD equations. Those equilibria with at least one pair of imaginary frequencies are linearly unstable while those with only real, nonzero frequencies are stable. There is a subset of equilibria having at least one pair of eigenmodes with frequency zero; this subset forms a two-dimensional boundary between these three-dimensional regions of stable and unstable equilibria.

It is not possible to distinguish between ideal and resistive instabilities in the low-dimensional system since there is no analog of the local field line constraints. Reconnection in this system cannot destroy flux since $\eta=0$. Thus an instability arises when the system may lower its energy through some combination of ideal motion and change in field line topology. When such a combination is energetically favorable in a full MHD system it seems likely that the ensuing plasma motion would give rise to enough turbulent motion to achieve the necessary reconnection.

During quasistatic evolution the system remains close to an equilibrium so its progress can be depicted as a trajectory in the space of equilibria, $\mathbf{J}^0$. It has been suggested for full MHD [10] and reduced MHD [2] that motion cannot remain quasistatic in the neighborhood of the neutrally stable boundary. At this point the system will abruptly relax to a new, stable equilibrium of lower magnetic energy, a process called "loss of equilibrium." The general features of this process can be elucidated using the low-dimensional model, and can be expected to pertain to both full MHD and reduced MHD.

Quasistatic evolution can start from any stationary equilibrium; here the arbitrary isovector $\mathbf{J}^0=(4.93,-2.63,-1.10)$ will be used to define the starting point. Rather than random footpoint motion the time-dependent vorticity isovectors $\mathbf{f}^0=(2t/\tau_0^2)(-2.07,-1.42,0)$ and $\mathbf{f}^1=(2t/\tau_0^2)(0.46,-3.52,0)$ will be used, where the parameter τ_0 must be chosen sufficiently large for the resulting motion to be quasistatic. With these conditions it is possible to integrate Eqs. (5) and (6) numerically using standard integration techniques. A typical solution in which $\nu=2$ and $\tau_0=50$ is shown in Fig. 1. The magnetic energy increases slowly from its initial value of $E_M=0.8$ to $E_M=1.2$ and then suddenly drops to $E_M=0.6$ at time $t\simeq 31$. Coincident with the drop in the magnetic energy the values of viscous power and kinetic energy (not shown) experience abrupt spikes lasting about three Alfvén times. At times before and after this spike the values of the kinetic energy remained below 3×10^{-4} times the magnetic energy; this is a strong indication that the system was evolving quasistatically.

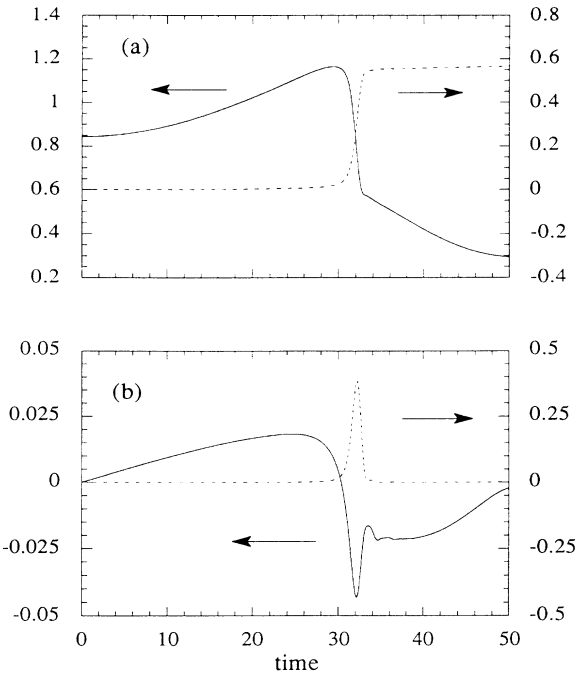

FIG. 1. Time histories from a single event. (a) Magnetic energy E_M (solid curve) and dissipated energy $\int dt\, P_\nu$ (dashed curve). (b) Footpoint power P_F (solid curve) and viscous dissipation rate P_ν (dashed curve).

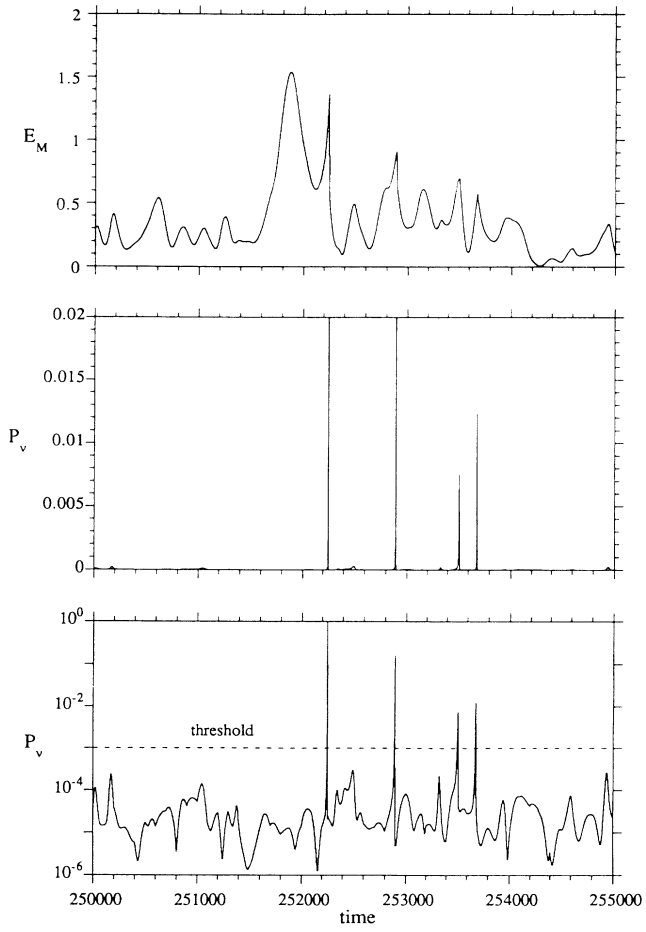

FIG. 2. Section of the time history of a long run with multiple impulsive events, showing magnetic energy E_M and both linear and logarithmic plots of the viscous dissipation rate P_ν.

The values of the isovector $\mathbf{J}^0$ during this run show a steady progression toward the stability boundary, terminating at a point very close to the boundary at $t=27$. At this time it is not possible to identify an equilibrium which the system is near. The quasistatic sequence resumes after $t=33$ at a point well inside the stable region. The difference in energies between the end of the first sequence and the beginning of the second sequence is $\Delta E_M \simeq 0.6$, consistent with the difference shown in Fig. 1.

Increasing the parameter τ_0 does not change the loss-of-equilibrium event just described. The time at which the event occurs scales with τ_0 and the kinetic energy before and after the event scales with τ_0^{-2}, but the peak value of P_ν and the net energy drop are unchanged. The energy drop is also independent of the viscosity ν; however, the value $\nu \simeq 2$ was found to minimize the time taken for a typical relaxation event.

Integrating Eqs. (5) and (6) for long times T with random footpoint driving yields sporadic loss-of-equilibrium events, each one similar to the one just studied but with a wide range of amplitudes. Since the driving is statistically stationary the system will find a statistical steady state. It is the properties of this statistical steady state that are of primary interest in this system and long runs provide a Monte Carlo approach to study them.

Figure 2 shows the section of one long run with $\nu=(2\pi)^2/20\simeq 2$, $\tau_E=300$, and $\tau_C=100$. The magnetic energy fluctuates continuously in response to the randomly varying footpoint motion, sometimes dropping abruptly as it did in the previous example. The viscous damping power has slow quasistatic fluctuations at levels around $\nu\tau_E^{-2}\sim 10^{-5}$, and short, strong relaxation spikes with amplitudes as high as $P_\nu=1$. These two components can be distinguished using a viscous power threshold; in this case we used $P_\nu=10^{-3}$. A single relaxation event is defined to begin when P_ν first exceeds this threshold and to end when it falls below the threshold for more than one Alfvén time.

During a full run of 10^6 Alfvén times, of which Fig. 2 is a section, there were 1093 such events. Figure 3(a) shows the distribution of amplitudes ΔE_M estimated by integrating $P_\nu(t)$ during the event. It shows that larger-amplitude events are less frequent, decreasing at a slope close to ΔE_M^{-1}. The lower cutoff of this distribution is due to the threshold used for detecting events. The amplitudes of events which peak just above the threshold are likely to be underestimated, leading to inaccuracies on the left of the plot.

The distribution of intervals between successive events, Δt, is shown in Fig. 3(b). These are exponentially distri-

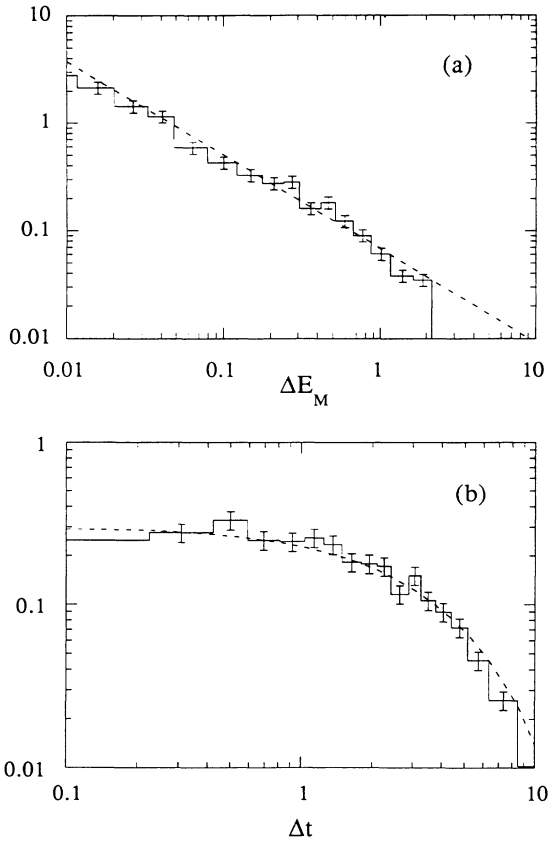

FIG. 3. Histograms from 1093 events. (a) Event amplitudes ΔE_M; dashed line is $0.068\Delta E_M^{-0.87}$. (b) Time interval between successive events, $\Delta t/\tau_E$; dashed line is $0.3\exp(-\Delta/3.3\tau_E)$.

buted with a mean value of 915 Alfvén times or about $3\tau_E$. In other runs with different values of τ_C and τ_E the mean interval remains about $3\tau_E$, independent of the correlation time τ_C. Exponential distributions are often associated with Poisson processes, that is, processes where the probability of an event does not depend on the time since the previous event. Since this system is driven by noise it is not surprising that it has such a property.

A scatter plot of Δt against ΔE_M for all 1093 events shows no apparent correlation. This would not be the case if the magnetic field built up energy continuously until it was released by a loss of equilibrium. Instead, the magnetic field both gains and loses energy randomly to the footpoints during the interval between events. This is possible because there are enough degrees of freedom for the system to change its relation to the footprints.

Thus, the dynamical state of a nonlinear, quasistatic but randomly driven system of many degrees of freedom passes quasistatically through many equilibrium configurations. Occasionally, two neighboring equilibria are separated by a finite difference of potential energy with no intervening barrier. The transition between these equilibria occurs on the fast dynamical time scale and results in an abrupt release of energy. A simple low-dimensional system provides a generic picture of such an event. When this low-dimensional system is driven continuously the statistics of its impulsive relaxation events is Poisson-like and their frequency varies as ΔE_M^{-1}, where ΔE_M is the energy released in a single event. It remains to be established that these statistical properties are common to systems of higher dimension.

We are grateful to Robert Rosner for discussions on this topic. This work was supported by NSF Grant No. 90-20719 and computations were performed at the Cornell National Supercomputing Center, supported by NSF and IBM.

[1] I. B. Bernstein, E. A. Frieman, M. D. Kruskal, and R. M. Kulsrud, Proc. R. Soc. London A **244**, 17 (1958).
[2] D. W. Longcope and R. N. Sudan, Astrophys. J. **384**, 305 (1992).
[3] See, for example, E. R. Priest, *Solar Magnetohydrodynamics* (Reidel, Boston, 1984).
[4] H. Hudson, Solar Phys. **133**, 357 (1991).
[5] E. N. Parker, Astrophys. J. **330**, 474 (1988).
[6] E. N. Parker, Astrophys. J. **174**, 494 (1972).
[7] H. Strauss, Phys. Fluids **19**, 134 (1976); M. N. Rosenbluth *et al.*, Phys. Fluids **19**, 1987 (1976).
[8] See, for example, J. Heyvaerts and E. R. Priest, Astron. Astrophys. **117**, 220 (1983).
[9] P. L. Similon and R. N. Sudan, Astrophys. J. **336**, 442 (1989).
[10] T. Gold, in *Proceedings of the AAS-NASA Symposium on the Physics of Solar Flares*, edited by W. N. Hess (NASA, Washington, DC, 1964), p. 389.